ARTICLE

Characterisation of Schiff base and chromophore in green proteorhodopsin by solid-state NMR

**Nicole Pfleger · Mark Lorch · Andreas C. Woerner ·
Sarika Shastri · Clemens Glaubitz**

Abstract The proteorhodopsin family consists of hundreds of homologous retinal containing membrane proteins found in bacteria in the photic zone of the oceans. They are colour tuned to their environment and act as light-driven proton pumps with a potential energetic and regulatory function. Precise structural details are still unknown. Here, the green proteorhodopsin variant has been selected for a chemical shift analysis of retinal and Schiff base by solid-state NMR. Our data show that the chromophore exists in mainly all-*trans* configuration in the proteorhodopsin ground state. The optical absorption maximum together with retinal and Schiff base chemical shifts indicate a strong interaction network between chromophore and opsin.

Keywords Proteorhodopsin · Solid-state NMR · Schiff base · Retinal

Mark Lorch and Andreas C. Woerner contributed equally to this work.

Electronic supplementary material The online version of this article (doi:10.1007/s10858-007-9203-5) contains supplementary material, which is available to authorized users.

N. Pfleger · M. Lorch · A. C. Woerner · S. Shastri ·
C. Glaubitz (✉)
Institute for Biophysical Chemistry, Centre for Biomolecular Magnetic Resonance, J. W. Goethe University, Max von Laue Str. 9, 60438 Frankfurt am Main, Germany
e-mail: glaubitz@em.uni-frankfurt.de

Present Address:
M. Lorch
Department of Chemistry, University of Hull, Hull, UK

Abbreviations

bR	Bacteriorhodopsin
PR	Proteorhodopsin
wt	Wild type
PSB	Protonated Schiff base
DA	Dark adapted
LA	Light adapted
MAS	Magic angle sample spinning

Introduction

Proteorhodopsin (PR) is a retinylidene membrane protein found in the genomes of many species of marine γ-proteobacteria in the oceans (Beja et al. 2000; Sabehi et al. 2005). Approximately 800 variants have been found so far which share 80% sequence identity but show different absorption maxima shifted by ~ 35 nm between green and blue PR (Wang et al. 2003). The green absorbing form (27 kDa, primary accession number Q9F7P4, $\lambda_{max} \sim 520$ nm) has been the focus of a number of studies. Based on comparison with bR, its 249 residues are predicted to be arranged in seven transmembrane helices. Green proteorhodopsin (PR) shares a 30% sequence identity with bacteriorhodopsin (bR). The primary proton acceptor D85, the proton donor D96, the Schiff base linkage K216 and the counterions of the Schiff base R82 and D212 in bR correspond to D97, E108, K231, R94 and D227 in PR, respectively. In contrast to bR, PR has no ionisable extracellular groups for a fast release of protons to the extracellular environment. The pK_a of the primary proton acceptor in PR is five pH units higher compared to bR (PR: $pK_{a,D97} \sim 7.2$, bR: $pK_{a,D85} \sim 2.5$). Outward driven proton pumping has been found at $pH > pK_{a,D97}$ but experiments

by Friedrich et al. have also shown an inversion at pH < $pK_{a,D97}$ (Friedrich et al. 2002). These findings suggest that PR could also have a regulatory function, but the proton acceptor is usually deprotonated under sea water conditions allowing the build up of an electrochemical potential. Considering the high abundance of PR, a very important role in the conversion of light energy to chemical energy in the photic zone of the oceans can be envisaged (Walter et al. 2007). PR undergoes a photocycle with a short turnover time of about 20 ms which contains K, M, N and O intermediates (Beja et al. 2000; Dioumaev et al. 2002). While the photocycle has been studied spectroscopically in some detail (Bergo et al. 2004; Dioumaev et al. 2002; Imasheva et al. 2005; Lenz et al. 2006, 2007; Varo et al. 2003; Wang et al. 2003), no structural data are available yet.

Here, we present a first solid-state NMR characterisation of chromophore and Schiff base of PR reconstituted into lipid bilayers. Solid-state NMR has been very extensively used to study its archaeal homologue bR, the best characterised membrane protein in terms of structure and function (for reviews see for example Lanyi and Schobert 2002; Luecke and Lanyi 2003). In fact it was the first membrane protein to be studied by solid-state NMR (Engelhard et al. 1990; Harbison et al. 1984; Kinsey et al. 1981). Therefore, an excellent knowledge base is available to which our data can be compared. Here, we report the ^{13}C chemical shifts of 10,11-^{13}C$_2$ retinal in PR and for comparison in bR. The number of resonance lines allows a direct assessment of the number of retinal populations within the protein. Their chemical shifts are valuable indicators for interactions within the binding pocket and could be used for quantum chemical calculations (Dreuw 2006). Our data show unambiguously an all-trans retinal conformation in dark adapted PR. We have also measured ^{15}N chemical shifts of the protonated Schiff base ^{15}N ζ-K231 in the wild type and upon a D97N single site mutation. This mutation emulates a photocycle intermediate state by keeping the primary proton acceptor in a "protonated" state. Comparing the relationship of the ^{15}N chemical shift and chromophore absorption maximum with those found in bR provides new insight into the PR retinal environment.

Materials and methods

Materials: All-trans-retinal was obtained from Sigma-Aldrich, unlabelled amino acids and nucleotide bases for the defined medium from AppliChem, ^{15}N ζ-lysine from Cambridge Isotopes, LB medium from Roth, 1-Palmitoyl-2-Oleoyl-sn-Glycero-3-Phosphocholine (POPC) and 1-Palmitoyl-2-Oleoyl-sn-Glycero-3-[Phospho-rac-(1-glycerol)] (POPG) from Avanti Polar Lipids. N-Dodecyl-β-D-maltosid

(DDM) was obtained from AppliChem, N-Octyl-ß-D-glucopyranoside (OG) from GLYCON Biochem. GmbH, Ni-NTA agarose from Qiagen and Biobeads (SM-2) from BioRad. The 10,11-^{13}C$_2$ all-trans retinal was kindly provided by M. H. Levitt, Southampton (Feng et al. 2000).

Preparation of [^{15}N ζ-Lys]-PR: Expression of PR (wt and D97N) was essentially done as described (Friedrich et al. 2002) but cells were grown in defined medium (Muchmore et al. 1989) with 50 μg/mL kanamycin until an OD$_{578}$ of 0.8 was reached. After spin-down, cells were resuspended in defined medium containing ^{15}N ζ-Lys. After 15 min of incubation, 1 mM IPTG and 0.7 mM of all-trans retinal were added. Cells were harvested after three hours of incubation.

Preparation of [10,11-^{13}C$_2$ Ret]-PR: LB medium was used instead of defined medium. Cells were induced by 1 mM IPTG when an OD$_{578}$ of 0.8 was reached. Simultaneously, 0.7 mM 10,11-^{13}C$_2$ all-trans retinal was added.

Purification: His-tagged PR was essentially purified as described by others (Hohenfeld et al. 1999) with only minor modifications (supporting information). An average protein yield of DDM solubilised PR of 10 mg/L culture was obtained (A$_{280}$/A$_{518}$ = 1.9).

Reconstitution: To prepare proteoliposomes, 1 mg of DDM solubilised protein (1 mg/ml) was added to 5 mg of lipids (molar ratio POPC:POPG = 5:1) dissolved in 1 ml buffer containing 300 mM NaCl, 50 mM MES, 2% OG, pH 6. After incubation for 1 h at room temperature, polystyrene beads were added for detergent removal for two hours at room temperature followed by incubation over night at 4°C. Detergent removal by dialysis and the use of total E. coli lipid mixture worked equally well. After centrifugation, the pellet was transferred to a 4 mm MAS rotor. Light adaption was performed by spreading the sample as a thin film and illuminating the sample with white light for 20 min at 150 W and subsequent freezing into liquid nitrogen.

Preparation of all-trans-[10,11-^{13}C$_2$ Ret]-bR took place as described before (Mason et al. 2005).

Optical spectroscopy: UV/VIS spectra of detergent solubilised PR were acquired on a Jasco V-550 spectrophotometer. Spectra at various pH values were taken in buffers containing 300 mM NaCl, 0.5% DDM including 20 mM Na-acetate (pH 4–5), 50 mM MES (pH 6), 50 mM HEPES (pH 7), 50 mM Tris (pH 8–9) or 50 mM phosphate buffer (pH 10–13).

^{13}C and ^{15}N MAS-NMR: Experiments were carried out on a Bruker Avance 600 equipped with a 4 mm MAS DVT probe head. Cross polarization experiments were performed at 60.88 MHz or 150.92 MHz for ^{15}N and ^{13}C, respectively. An 80–100% ramped proton pulse of 0.5 ms for ^{15}N and 1.0 ms for ^{13}C was used during the Hartmann–Hahn match. Proton decoupling (Fung et al. 2000) of

typically 90 kHz was applied during a 50 ms acquisition time. The recycle delay time was 2 s. Spectra were referenced externally to the ^{15}N resonance of solid ^{15}N ammonium sulphate at 27 ppm and to the ^{13}C signal of TMS at 0 ppm. All measurements were carried out at sample spinning of 10 kHz at 210 K. ^{13}C double-quantum filtering was achieved by using a POST-C7 experiment with 110 kHz decoupling during 457 μs double-quantum excitation and reconversion (Lee et al. 1995). An amount of 4–6 mg of protein was used per sample and 30–40 k scans were acquired per experiment.

Results and discussion

^{13}C chemical shifts of 10,11-$^{13}C_2$ retinal in PR

^{13}C MAS NMR spectra of PR with 10,11-$^{13}C_2$ retinal reconstituted in lipid bilayers are shown in Fig. 1. For dark adapted PR, two signals are detected at 138.5 and 130 ppm (Fig. 1a). For comparison, we have carried out the same experiment on dark adapted bR (Fig. 1c). Here, due to the *cis-trans* isomerisation equilibrium of the chromophore, four resonances are found, which can be assigned to all-*trans*-C_{11}, 13-*cis*-C_{11}, all-*trans*-C_{10} and 13-*cis*-C_{10} (Harbison et al. 1985).

The chemical shifts of both peaks in PR are within the range expected for C_{11} and C_{10}, based on the comparison with model compounds, with bR and with rhodopsin (Han et al. 1993; Harbison et al. 1985). In retinal, all odd-numbered carbon positions are always less shielded than even ones (Bremser and Paust 1974). Therefore, we assign the resonances at 138.5 and 130 ppm to C_{11} and C_{10}, respectively. The line widths of the C_{11} and C_{10} peaks are 3 and 2 ppm. Their differences could be caused by a small retinal heterogeneity or stronger coupling to adjacent protons of C_{11}. The fact that only two peaks are observed instead of four shows unambiguously that ground state PR contains only all-*trans* retinal. In previous extraction experiments, where the retinal is studied outside the protein, all-*trans* mixed with 5% (Imasheva et al. 2005) or 20% (Friedrich et al. 2002) 13-*cis* retinal had been found. Our results are also supported by FTIR and Raman data which had been interpreted in favour of a predominantly all-*trans* retinal population (Bergo et al. 2004; Dioumaev et al. 2002; Imasheva et al. 2005).

Extensive studies on retinal protonated Schiff base model compounds have been carried out in order to identify factors which influence ^{13}C chemical shifts and absorption maxima of the chromophore (Albeck et al. 1992; Hu et al. 1994). It has been found that λ_{max} increases with the chemical shifts of odd numbered carbons (Albeck et al. 1992). Comparing the C_{11} chemical shifts of all-*trans*
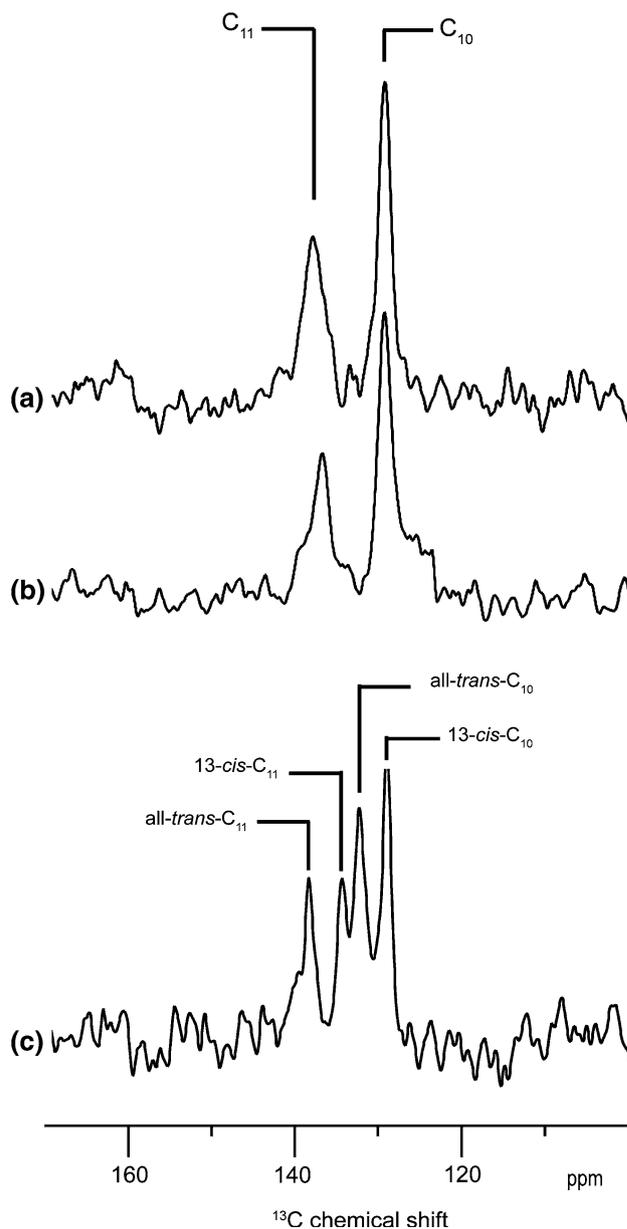
Fig. 1 Double quantum filtered ^{13}C MAS spectra of PR (**a, b**) and bR (**c**) with 10,11-$^{13}C_2$ retinal. Dark adapted PR shows two well resolved resonances at 130 and 138.5 ppm which can be assigned to C_{10} and C_{11} (**a**). Two small shoulders appear upon light adaptation, but chemical shifts and intensities of both main resonances are not significantly altered (**b**). In contrast, dark adapted bR shows four resonances at 139.1, 135.1, 133 and 129.7 ppm which correspond to all-*trans*-C_{11}, 13-*cis*-C_{11}, all-*trans*-C_{10} and 13-*cis*-C_{10}, respectively

retinal in bR and PR (bR: 139.1, PR: 138.5 ppm) with their absorption maxima (bR: 568 nm, PR: ca. 520 nm) shows that they follow this trend but also deviate significantly from the model compounds. These differences are most likely caused by the steric interactions with residues in the binding pocket and their effects onto the retinal structure, the retinal ring orientation (6s-*cis* or 6s-*trans*), the effects

of charges, or differences in the effective electricity constant within the retinal environment. However, the individual contributions of these factors must be addressed by further solid-state NMR experiments.

C_{10} chemical shifts are less dependent on the parameters mentioned above, but the difference between bR and PR is significantly larger (3 ppm) than for C_{11} (0.6 ppm). This could be explained by a different chemical environment such as a tighter binding pocket: Although PR shares a general 30% sequence identity (70% in binding pocket) with bR, important differences exist such as the high pK_a of D97 and the presence of a highly conserved His-75 close to the retinal binding pocket.

Upon light adaption, a slight broadening of the baseline with two small shoulders at 139.9 and 125.8 ppm is observed (Fig. 1b). This could be due to conformational changes of a small fraction of the retinal. Resonance Raman spectra did also provide evidence for an almost entirely all-*trans* retinal conformation in light adapted PR (Dioumaev et al. 2002; Krebs et al. 2003).

## ^{15}N chemical shifts of the protonated Schiff base
^{15}N ζ-K231 in PR

As shown for bR, ^{15}N ζ chemical shifts of the Schiff base also report on the retinal conformation (Harbison et al. 1983; Hu et al. 1997b). We have therefore inspected the ^{15}N chemical shift of the protonated Schiff base at K231. The ^{15}N CP MAS spectrum of dark adapted ^{15}N ζ-lys PR is shown in Fig. 2a. A single resonance of the protonated Schiff base is found at 186 ppm while all other ^{15}N ζ-lys resonate at 37 ppm. The spectrum does not change upon light adaption (Suppl. Material). In dark adapted bR, the protonated Schiff base is found at 171 ppm for all-*trans* and at 178 ppm for 13-*cis* retinal, which changes to a single resonance at 171 ppm upon illumination (re-referenced to solid ammonium sulphate) (Harbison et al. 1983). It is intriguing to note that the chemical shift in PR is similar to bovine rhodopsin (Creemers et al. 1999), but this seems merely a coincidence considering the differences in retinal conformations, protein sequence and evolutionary origin. The spectral resolution obtainable in our samples is comparable to purple membrane preparations and should be sufficient to resolve different species in PR, if they did exist. As this is not the case, our ^{15}N measurement supports the conclusion of a predominantly all-*trans* conformation of the retinal, which was drawn from our ^{13}C data. Compared to bR, the protonated Schiff base in PR is less shielded. Based on a large number of Schiff base chemical shifts (δ) from all-*trans* retinylidene model compounds with both 6s-*cis* and 6s-*trans* ring orientation, an empirical relationship with the distance from the Schiff base (d) to
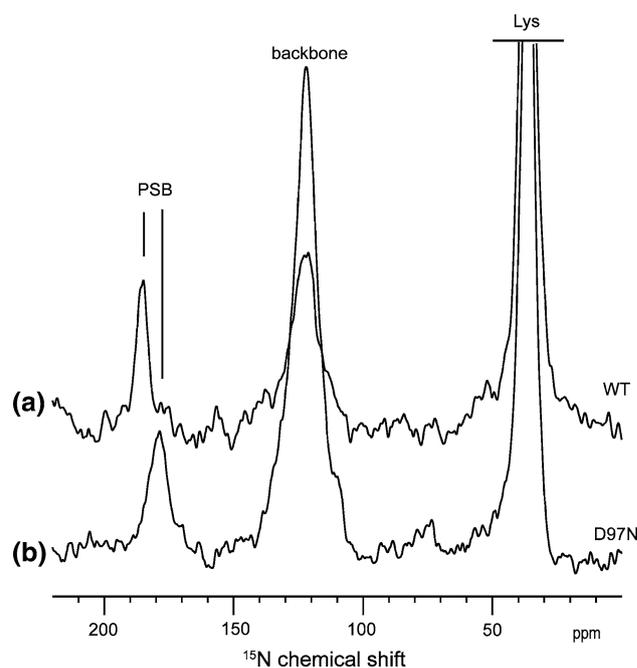
Fig. 2 ^{15}N CP spectrum of wt [^{15}N ζ-Lys] PR at pH 9 (**a**) and D97N [^{15}N ζ-Lys] PR at pH 6 (**b**). The ^{15}N ζ-Lys$_{231}$ resonance changes from 186 ppm in wt PR to 179ppm in D97N

the counterions and the absorption maximum (λ_{max}) in form of $\delta \sim 1/d^2 \sim 1/\lambda_{max}$ had been found which agrees very well with bR (Hu et al. 1997a) but differs for PR (Fig. 3). Based on the larger chemical shift in PR compared to bR, a stronger counterion interaction (i.e., a shorter effective distance) should be expected. For example, an outward movement of the arginine (R94) side chain in PR compared to bR (R82) would weaken the interaction between R94 and D97 and thus strengthen the coupling of D97 and the protonated Schiff base (PSB) (Krebs et al. 2003). When comparing the correlation between chemical shifts and λ_{max} (Fig. 3), an absorption maximum of 480 nm (20833 cm^{-1}) is predicted while $\sim$520 nm (19231 cm^{-1}) in detergent and 545 nm (18349) in the reconstituted samples were actually observed. Additional factors must contribute to this red shift, such as twisting around double bonds within the retinal (Hu et al. 1997a) or negative charges close to the chromophore (Hu et al. 1994). Indeed, homology modelling of PR onto bR (1C3W) (Friedrich et al. 2002) reveals the location of a negative charged D142 within a distance of 8 Å to the retinal. The corresponding residue in bR, A126, is neutral.

A monotonic relationship had been described for the principal values σ_{33} and σ_{22} of the ^{15}N chemical shift anisotropy tensor of the PSB in model compounds and bR$_{568}$ (de Groot et al. 1989). Using low speed MAS, we were also able to determine the ^{15}N chemical shift anisotropy to –132 ppm with an asymmetry parameter of
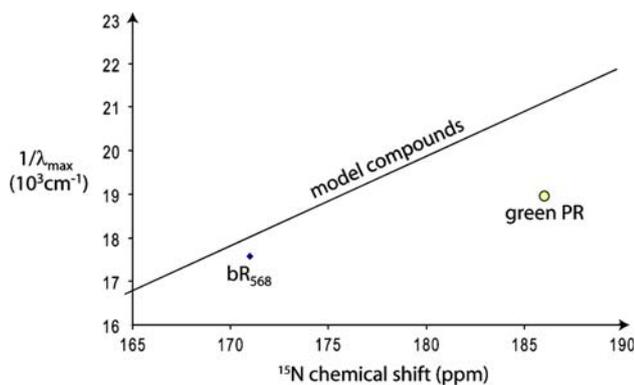
Fig. 3 Protonated Schiff bases of retinal derivatives with *all-trans* polyene chains and 6s-cis and 6s-trans ring conformations with different halide counterions show a proportional relationship of the maximum wavelength and the ^{15}N chemical shift of the PSB. Proteorhodopsin shows a much stronger deviation from this relationship than *all-trans* bR (bR$_{568}$). The figure was adopted from (Hu et al. 1994)

0.73 (σ_{11} = 54 ppm, σ_{22} = 203 ppm, σ_{33} = 300 ppm, Fig. 4). This is similar to bR but σ_{33}/σ_{22} deviates from the empirical rule most likely due to a stronger network of couplings around the Schiff base as discussed above. Furthermore, FTIR and Raman studies suggest a strong hydrogen coupling network between chromophore and adjacent residues or water molecules, which could also contribute to the chemical shift and λ_{max} differences between PR and bR (Ikeda et al. 2007) (Fig. 3).

A comparison of UV/VIS absorption spectra with ^{15}N MAS NMR data is shown in Fig. 5 for different pHs. For wild type PR, λ_{max} shifts from 545 nm at pH 4 to 516 nm at pH 9, which is thought to be mainly due to the deprotonation of D97 (Friedrich et al. 2002). At the same time, the Schiff base chemical shifts and signal intensities remain almost constant between pH 6 and 11 (Fig. 5a). Below pH6 and above pH12 resonance line broadening has been observed. Signals for the deprotonated Schiff base could only been detected for pH > 12 where the protein starts to denature. Schiff base deprotonation is seen in the UV/VIS spectra where an additional absorption maximum at 366 nm above pH12 occurs (Imasheva et al. 2004). The high pH stability of K231 could be explained with a high dielectric constant potentially resulting from a water cluster which could stabilize the PSB. Indeed, recent FTIR data suggests a strongly hydrogen bonded water cluster in alkaline PR (Ikeda et al. 2007).

The ^{15}N CP MAS spectrum of the ^{15}N ζ-lys labelled D97N mutant differs from the wild type as the Schiff base resonance is found at 179 ppm and a general broadening is observed (Fig. 5b) which is most likely caused by an altered counterion interaction (Hatcher et al. 2002). The absorption maximum λ_{max} is found at 560 nm between pH 4 and 9 and shifts to 400 nm above pH 9 at which also the
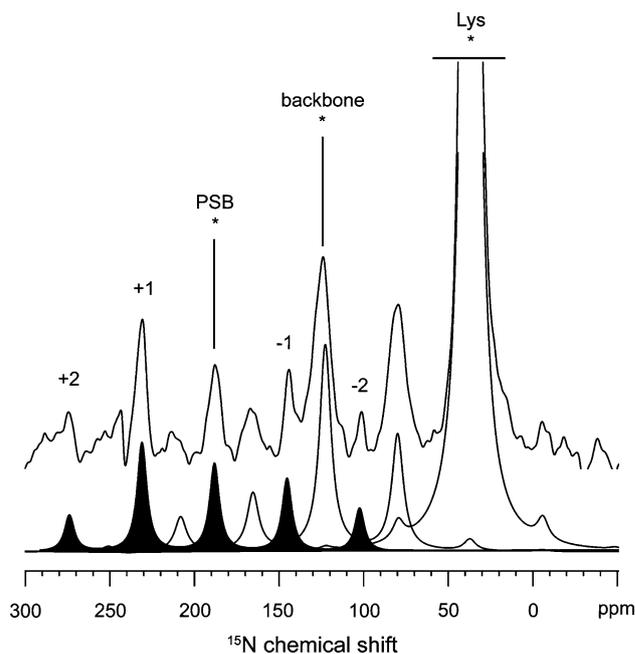

Fig. 4 ^{15}N CP-MAS spectrum of wt [^{15}N ζ-Lys] PR (pH 9) at 3.3 kHz sample spinning at 60.88 MHz. The spectrum decays into spinning sideband families of the Schiff base, lysine side chains and amide backbone. Their isotropic signals are labelled with (*). Indices describe the PSB spinning sidebands. The spectrum was deconvoluted and fitted against a calculated sideband pattern using Topspin 2.0 (Bruker, Karlsruhe). For the protonated Schiff base (black), a chemical shift anisotropy of –132 ppm with η = 0.73 was found (σ_{11} = 54 ppm, σ_{22} = 203 ppm, σ_{33} = 300 ppm, fitting error 10%)

^{15}N resonance starts to decay (Fig. 5b). The formation of such an M-like state is also supported by the observation of a downfield shifted peak at 306 ppm (data not shown) corresponding to the deprotonated Schiff base. Therefore, the D97N mutant could potentially offer the opportunity to study functional and structural properties of the M-like state in the PR photocycle by solid-state NMR.

Summary

The ^{13}C chemical shifts of 10,11-^{13}C$_2$ retinal and the ^{15}N chemical shift of the protonated Schiff base K231 in green proteorhodopsin show unambiguously that ground state PR only contains all-*trans* retinal. The C$_{10}$ and C$_{11}$ are more shielded in PR compared to bR. The large ^{15}N chemical shift of 186 ppm of the protonated Schiff base indicates a strong counterion interaction, while additional charges or constraints on the retinal conformation are needed to explain the absorption maximum. In contrast to bR, residue D142 adjacent to the chromophore could cause an additional charge effect. The existence of a strong coupling network in the Schiff base vicinity is also supported by the high pH stability of the PSB chemical shift, which is

Fig. 5 Correlation of UV/VIS with ^{15}N ζ-Lys$_{231}$ CP spectra of wt (**a**) and PR D97N (**b**) at different pH values. In wt PR, the ^{15}N signal of the PSB remains relatively constant over a pH range from 6 to 11 suggesting that the Schiff base remains mainly in its protonated form. The deprotonated form at 300 ppm could not be observed below pH 12. However, a peak at 366 nm starts occurring at pH 11 indicting deprotonation of the Schiff base. The acidic form and the basic form of the ground state appear at 545 and 516 nm respectively. For the D97N mutant, a decrease of the ^{15}N signal of the PSB occurs at high pH. This reveals the formation of an M-like state with a deprotonated SB which is also seen in the UV-VIS spectrum where an M-state signal at 400 nm occurs. Between pH 5 and 9, the mutant seems to be trapped in an N-like state as ^{15}N chemical shift and λ_{max} correspond to a protonated Schiff base. The pK$_a$ for D97N PR was determined to be 9.7
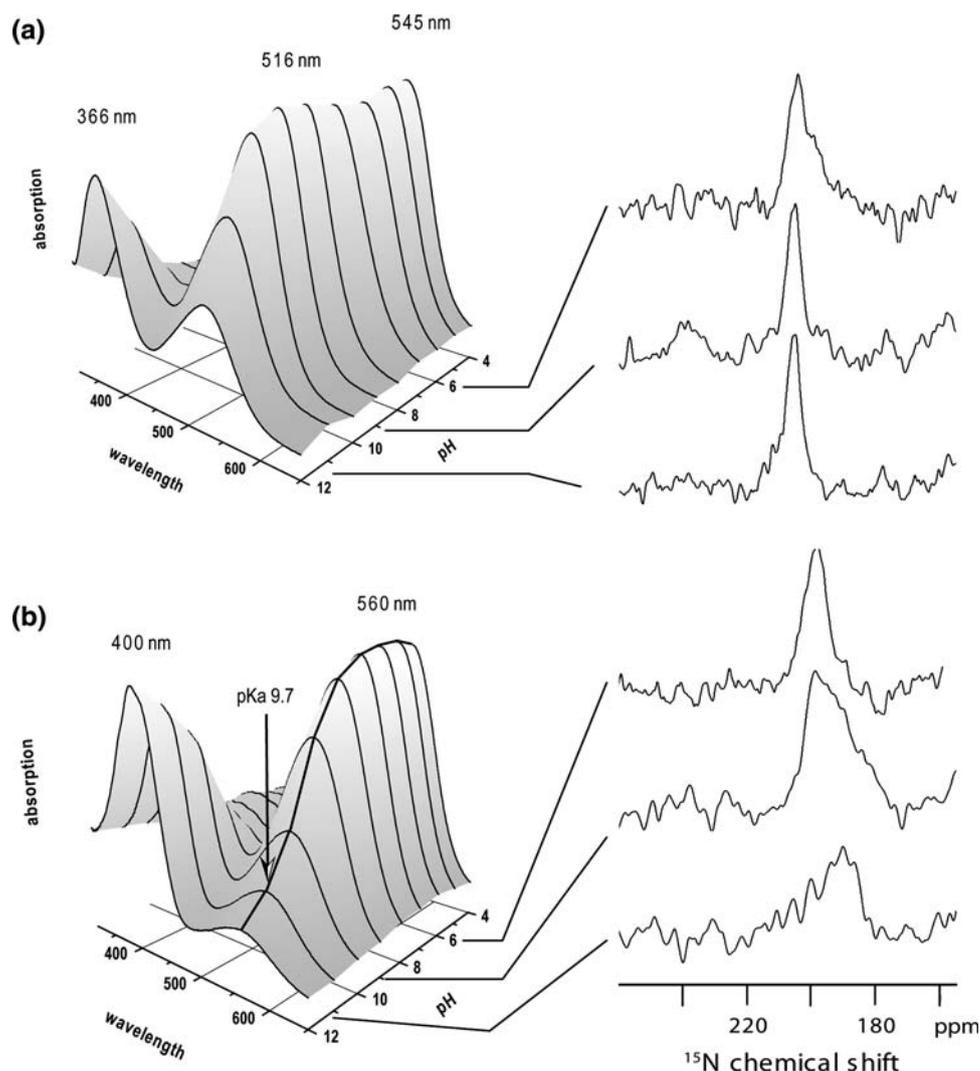
weakened in the D97N mutant. The pK$_a$ of the Schiff base in the D97N mutant is decreased compared to the wild type. Considering the fact that the pK$_a$ of the proton acceptor in PR is 5 pH units higher than in bR, different interaction strength with the Schiff base is expected. Unfortunately, our data do not allow a direct conclusion about the retinal ring orientation in PR. This question can be answered by further solid-state NMR experiments, but it is interesting to note that in other prokaryotic rhodopsins such as bacteriorhodopsin (Luecke et al. 1999), halorhodopsin (Kolbe et al. 2000) and sensory rhodopsin II (Luecke et al. 2001), the all-trans retinal polyene chain is always coplanar with the beta-ionone ring, which is in the 6s-trans conformation. The interactions of Schiff base and retinal with opsin will be further studied by solid-state NMR using multiple amino acid labelling.

References

Albeck A, Livnah N, Gottlieb H, Sheves M (1992) C-13 Nmr-studies of model compounds for bacteriorhodopsin—factors affecting the retinal chromophore chemical-shifts and absorption maximum. J Am Chem Soc 114:2400–2411

Beja O, Aravind L, Koonin EV, Suzuki MT, Hadd A, Nguyen LP, Jovanovich SB, Gates CM, Feldman RA, Spudich JL, Spudich EN, DeLong EF (2000) Bacterial rhodopsin: evidence for a new type of phototrophy in the sea. Science 289:1902–1906

Bergo V, Amsden JJ, Spudich EN, Spudich JL, Rothschild KJ (2004) Structural changes in the photoactive site of proteorhodopsin during the primary photoreaction. Biochemistry 43:9075–9083

Bremser W, Paust J (1974) C-13 Nmr-spectrum of beta-carotene and charge-distribution in poly chain of apocarotinals. Org Magn Resonance 6:433–435

Creemers AFL, Klaassen CHW, Bovee-Geurts PHM, Kelle R, Kragl U, Raap J, de Grip WJ, Lugtenburg J, de Groot HJM (1999) Solid state 15N NMR evidence for a complex Schiff base

counterion in the visual G-protein-coupled receptor rhodopsin. Biochemistry 38:7195–7199

de Groot HJM, Harbison GS, Herzfeld J, Griffin RG (1989) Nuclear magnetic-resonance study of the Schiff-base in bacteriorhodopsin—counterion effects on the N-15 shift anisotropy. Biochemistry 28:3346–3353

Dioumaev AK, Brown LS, Shih J, Spudich EN, Spudich JL, Lanyi JK (2002) Proton transfers in the photochemical reaction cycle of proteorhodopsin. Biochemistry 41:5348–5358

Dreuw A (2006) Quantum chemical methods for the investigation of photoinitiated processes in biological systems: theory and applications. Chemphyschem 7:2259–2274

Engelhard M, Hess B, Metz G, Kreutz W, Siebert F, Soppa J, Oesterhelt D (1990) High-resolution C-13-solid state Nmr of bacteriorhodopsin—assignment of specific aspartic acids and structural implications of single site mutations. Eur Biophys J 18:17–24

Feng X, Verdegem PJE, Eden M, Sandstrom D, Lee YK, Bovee-Geurts PHM, de Grip WJ, Lugtenburg J, de Groot HJM, Levitt MH (2000) Determination of a molecular torsional angle in the metarhodopsin-I photointermediate of rhodopsin by double-quantum solid-state NMR. J Biomol Nmr 16:1–8

Friedrich T, Geibel S, Kalmbach R, Chizhov I, Ataka K, Heberle J, Engelhard M, Bamberg E (2002) Proteorhodopsin is a light-driven proton pump with variable vectoriality. J Mol Biol 321:821–838

Fung BM, Khitrin AK, Ermolaev K (2000) An improved broadband decoupling sequence for liquid crystals and solids. J Magn Reson 142:97–101

Han M, Dedecker BS, Smith SO (1993) Localization of the retinal protonated Schiff-base counterion in rhodopsin. Biophys J 65:899–906

Harbison GS, Herzfeld J, Griffin RG (1983) Solid-state N-15 nuclear magnetic-resonance study of the Schiff-base in bacteriorhodopsin. Biochemistry 22:1–5

Harbison GS, Smith SO, Pardoen JA, Courtin JML, Lugtenburg J, Herzfeld J, Mathies RA, Griffin RG (1985) Solid-state C-13 Nmr detection of a perturbed 6-S-trans chromophore in bacteriorhodopsin. Biochemistry 24:6955–6962

Harbison GS, Smith SO, Pardoen JA, Mulder PPJ, Lugtenburg J, Herzfeld J, Mathies R, Griffin RG (1984) Solid-state C-13 Nmr-studies of retinal in bacteriorhodopsin. Biochemistry 23:2662–2667

Hatcher ME, Hu JGG, Belenky M, Verdegem P, Lugtenburg J, Griffin RG, Herzfeld J (2002) Control of the pump cycle in bacteriorhodopsin: mechanisms elucidated by solid-state NMR of the D85N mutant. Biophys J 82:1017–1029

Hohenfeld IP, Wegener AA, Engelhard M (1999) Purification of histidine tagged bacteriorhodopsin, pharaonis halorhodopsin and pharaonis sensory rhodopsin II functionally expressed in Escherichia coli. Febs Lett 442:198–202

Hu JG, Griffin RG, Herzfeld J (1994) Synergy in the spectral tuning of retinal pigments: complete accounting of the opsin shift in bacteriorhodopsin. Proc Natl Acad Sci USA 91:8880–8884

Hu JGG, Griffin RG, Herzfeld J (1997a) Interactions between the protonated Schiff base and its counterion in the photointermediates of bacteriorhodopsin. J Am Chem Soc 119:9495–9498

Hu JGG, Sun BQQ, Petkova AT, Griffin RG, Herzfeld J (1997b) The predischarge chromophore in bacteriorhodopsin: a N-15 solid-state NMR study of the L photointermediate. Biochemistry 36:9316–9322

Ikeda D, Furutani Y, Kandori H (2007) FTIR study of the retinal Schiff base and internal water molecules of proteorhodopsin. Biochemistry 46:5365–5373

Imasheva ES, Balashov SP, Wang JM, Dioumaev AK, Lanyi JK (2004) Selectivity of retinal photoisomerization in proteorhodopsin is controlled by aspartic acid 227. Biochemistry 43:1648–1655

Imasheva ES, Shimono K, Balashov SP, Wang JM, Zadok U, Sheves M, Kamo N, Lanyi JK (2005) Formation of a long-lived photoproduct with a deprotonated Schiff base in proteorhodopsin, and its enhancement by mutation of Asp227. Biochemistry 44:10828–10838

Kinsey RA, Kintanar A, Oldfield E (1981) Dynamics of amino-acid side-chains in membrane-proteins by high-field solid-state deuterium nuclear magnetic-resonance spectroscopy—phenylalanine, tyrosine, and tryptophan. J Biol Chem 256:9028–9036

Kolbe M, Besir H, Essen LO, Oesterhelt D (2000) Structure of the light-driven chloride pump halorhodopsin at 1.8 A resolution. Science 288:1390–1396

Krebs RA, Dunmire D, Partha R, Braiman MS (2003) Resonance Raman characterization of proteorhodopsin's chromophore environment. J Phys Chem B 107:7877–7883

Lanyi JK, Schobert B (2002) Crystallographic structure of the retinal and the protein after deprotonation of the Schiff base: the switch in the bacteriorhodopsin photocycle. J Mol Biol 321:727–737

Lee YK, Kurur ND, Helmle M, Johannessen OG, Nielsen NC, Levitt MH (1995) Efficient dipolar recoupling in the Nmr of rotating solids—a sevenfold symmetrical radiofrequency pulse sequence. Chem Phys Lett 242:304–309

Lenz MO, Huber R, Schmidt B, Gilch P, Kalmbach R, Engelhard M, Wachtveitl J (2006) First steps of retinal photoisomerization in proteorhodopsin. Biophys J 91:255–262

Lenz MO, Woerner AC, Glaubitz C, Wachtveitl J (2007) Photoisomerization in proteorhodopsin mutant D97N. Photochem Photobiol 83:226–231

Luecke H, Lanyi JK (2003) Structural clues to the mechanism of ion pumping in bacteriorhodopsin. Adv Protein Chem 63:111–130

Luecke H, Schobert B, Lanyi JK, Spudich EN, Spudich JL (2001) Crystal structure of sensory rhodopsin II at 2.4 angstroms: insights into color tuning and transducer interaction. Science 293:1499–1503

Luecke H, Schobert B, Richter HT, Cartailler JP, Lanyi JK (1999) Structure of bacteriorhodopsin at 1.55 A resolution. J Mol Biol 291:899–911

Mason AJ, Turner GJ, Glaubitz C (2005) Conformational heterogeneity of transmembrane residues after the Schiff base reprotonation of bacteriorhodopsin—N-15 CPMAS NMR of D85N/T170C membranes. Febs J 272:2152–2164

Muchmore DC, Mcintosh LP, Russell CB, Anderson DE, Dahlquist FW (1989) Expression and N-15 labeling of proteins for proton and N-15 nuclear-magnetic-resonance. Method Enzymol 177:44–73

Sabehi G, Loy A, Jung KH, Partha R, Spudich JL, Isaacson T, Hirschberg J, Wagner M, Beja O (2005) New insights into metabolic properties of marine bacteria encoding proteorhodopsins. Plos Biol 3:1409–1417

Varo G, Brown LS, Lakatos M, Lanyi JK (2003) Characterization of the photochemical reaction cycle of proteorhodopsin. Biophys J 84:1202–1207

Walter JM, Greenfield D, Bustamante C, Liphardt J (2007) Light-powering Escherichia coli with proteorhodopsin. Proc Natl Acad Sci USA 104:2408–2412

Wang WW, Sineshchekov OA, Spudich EN, Spudich JL (2003) Spectroscopic and photochemical characterization of a deep ocean proteorhodopsin. J Biol Chem 278:33985–33991